Available online at www.sciencedirect.com
SCIENCE DIRECT
Catalysis Today 105 (2005) 66–73
CATALYSIS TODAY
www.elsevier.com/locate/cattod

Trends in the chemical properties of early transition metal carbide surfaces: A density functional study

John R. Kitchin [a], Jens K. Nørskov [b], Mark A. Barteau [a], Jingguang G. Chen [a,*]

[a] Center for Catalytic Science and Technology, Department of Chemical Engineering, University of Delaware, Newark, DE 19716, USA
[b] Center for Atomic-scale Materials Physics and Department of Physics, Technical University of Denmark, DK-2800 Lyngby, Denmark

Available online 6 June 2005

Abstract

In this paper we present density functional theory (DFT) investigations of the physical, chemical and electronic structure properties of several close-packed surfaces of early transition metal carbides, including β-Mo_2C(0 0 0 1), and the (1 1 1) surfaces of TiC, VC, NbC, and TaC. The results are in excellent agreement with experimental values of lattice constants and bulk moduli. The adsorption of atomic hydrogen is used as a probe to compare the chemical properties of various carbide surfaces. Hydrogen adsorbs more strongly to the metal-terminated carbide surfaces than to the corresponding closest-packed pure metal surfaces, due to the tensile strain induced in the carbide surfaces upon incorporation of carbon into the lattice. Hydrogen atoms were found to adsorb more weakly on carbide surfaces than on the corresponding closest-packed pure metal surfaces only when there were surface carbon atoms present, and in some cases very stable C–H species were formed. The DFT results indicated that the hydrogen adsorption energy could be correlated to the d-band center of the carbide surfaces, although the correlation was not as good as our previous studies on bimetallic surfaces.

Keywords: Metal carbides; DFT modeling; Electronic properties

1. Introduction

Early transition metal carbides and nitrides are among the hardest and most refractory materials known [1]. They have also gathered attention as potential catalysts since their ''platinum-like behavior'' was reported by Levy and Boudart [2]. In that work, ''platinum-like behavior'' referred specifically to three types of catalytic activity that are unique to Pt-group metals: (1) the oxidation of H_2 to form water, (2) the reduction of WO_3 by moist hydrogen, and (3) the isomerization of 2,2-dimethylpropane to 2-methylbutane. It was suggested in this seminal paper that carbon must change the electron distribution of the tungsten atoms in a manner that makes them more platinum-like. Since then, many studies and reviews have been reported on the electronic and structural properties of carbide surfaces [3] and their catalytic properties [4–6].

The purpose of the present work is to investigate the electronic structure of early transition metal carbide surfaces, in particular how their electronic structures are modified compared to those of the parent metal surfaces, and how these changes affect the chemical properties of these surfaces. The paper begins with a density functional theory (DFT) investigation of bulk β-Mo_2C and β-Mo_2C(0 0 0 1) surfaces. This is followed by the results of a DFT study of the electronic and chemical properties of the (1 1 1) surfaces of TiC, VC, NbC, and TaC.

2. Theoretical studies of β-Mo_2C

2.1. Bulk properties

Below 1500 K, mixtures of Mo- and C exist in the following phases: Mo, α-Mo_2C, β-Mo_2C and C, depending on the relative amounts of the two components [7]. We chose β-Mo_2C as a representative carbide phase for this work. The β-Mo_2C phase has an orthorhombic crystal structure, with $a = 6.022$ Å, $b = 4.725$ Å, and $c = 5.195$ Å [8]. The (1 0 0) surface corresponds to the closest-packed surface, and it can

* Corresponding author.
E-mail address: jgchen@udel.edu (J.G. Chen).

0920-5861/$ – see front matter © 2005 Elsevier B.V. All rights reserved.
doi:10.1016/j.cattod.2005.04.008

Table 1
Lattice constants for β-Mo_2C

Lattice parameter	Experimental [8]	Calculated	Difference (%)
a	6.022	6.129	1.8
b	4.725	4.805	1.7
c	5.204	5.298	1.8

be either Mo or C-terminated. Although the crystal structure is orthorhombic, the arrangement of Mo atoms is only slightly distorted from an hcp arrangement. Thus, the crystal structure can be loosely described as an hcp arrangement of Mo atoms, with carbon atoms occupying one-half of the octahedral interstitial sites. This has resulted in many reports referring to the closest-packed surface as the (0 0 0 1) surface. Although it is incorrect, it is convenient to keep this notation for consistency with the literature.

The DFT lattice parameters for β-Mo_2C were determined by minimizing the total energy of the unit cell with respect to the length of the lattice vectors using a Newton–Raphson scheme developed for that purpose. The experimentally known crystal structure was used as the initial starting point for the optimization. Complete internal relaxation was allowed at each step. DACAPO [9], which uses planewaves and ultrasoft pseudopotentials, was used for all calculations in this paper. A planewave cutoff of 350 eV, a $4 \times 4 \times 4$ Monkhorst Pack k-point grid, and the PW91 exchange-correlation functional were used in the optimization. The results are listed in Table 1. Each of the lattice parameters was overestimated by 1.5–2%. This is consistent with errors for pure transition metals; the calculated lattice constants for Mo and Pt were larger by 1.3 and 2.3%, respectively. Liu et al. recently determined the lattice constants of α-Mo_2C using $DMol^3$ [10], which uses a localized basis set rather than planewaves. Their results are also within ±2% of the experimental values. The bulk β-Mo_2C lattice parameters were determined for later use in investigations of surface properties, described in the next section.

2.2. Surface properties

The β-Mo_2C(0 0 0 1) was chosen as a model surface for a close-packed β-Mo_2C substrate. The surfaces were modeled by slabs separated by vacuum, using the DFT lattice parameters listed in Table 1. Each slab was two unit cells thick (four layers of Mo atoms and four layers of C atoms). Two of the layers were allowed to fully relax, and the other two layers were frozen at the bulk lattice parameters. A $4 \times 4 \times 1$ Monkhorst-Pack k-point setup was used. The planewave cutoff was set at 350 eV, and the PW91 exchange-correlation functional was used. The slabs were separated by three unit cells of vacuum and were further decoupled by use of a dipole correction scheme. Atom-projected densities of states (DOS) were calculated by projection of the one-electron states onto spherical harmonic atomic orbitals centered on atomic sites. Two projections were obtained, one with a cutoff radius at 1 Å to minimize contributions from neighboring sites, hereafter referred to as the short cutoff radius. The other result used no cutoff radius, hereafter referred to as the infinite cutoff radius. It has not been important to differentiate between these two radii in previous works examining electronic structures of metals and bimetallic surfaces in our research groups, but in this work it was found to be important, as will be discussed later.

The calculated electronic d-band structures of β-Mo_2C(0 0 0 1) surfaces were compared with those of Mo(1 1 0) and Pt(1 1 1), shown in Fig. 1. The surface d-band of both C- and Mo-terminated carbide surfaces appears broader than that of Mo(1 1 0). There are several new features in the Mo d-band structure of the carbide surface. Most obviously, there is a new peak around −12 eV in both the Mo- and C-terminated surfaces, and a second peak around −10 eV on the C-terminated surface. Both carbide d-bands show a shoulder between about −7 and −5 eV that is absent for the Mo(1 1 0) surface. These new features can be associated directly with hybridization between the d-orbitals and the carbon sp-orbitals. More specifically, the peak near −12 eV can be attributed to interactions between the surface Mo atoms and subsurface C atoms. This is illustrated in Fig. 2, where the s and p-bands of C atoms in the second layer are compared with the surface Mo atom d-band. The overlap of the peaks clearly identifies the feature near −12 eV as an interaction between the C s-orbitals and Mo d-orbitals. An interaction between the Mo d-orbitals and the subsurface carbon p-orbitals is responsible for the broadened shoulder between −5 and −7 eV. Fig. 2 shows the results of the atom-projected DOS for the infinite cutoff radius. The same conclusions were reached for the short cutoff radius results.

The second peak in the C-terminated surface at −10 eV is due to interactions between the surface Mo d-orbitals and the s-orbitals of the carbon atoms on the surface. The surface C s and p-bands closely resemble the subsurface C s and p-bands, but they are higher in energy due to their lower coordination compared to carbon in the bulk. Consequently, all of the resonances with the surface d-band are shifted to higher energy, as illustrated in Fig. 3. The same conclusions were reached if the short cutoff radius was used.

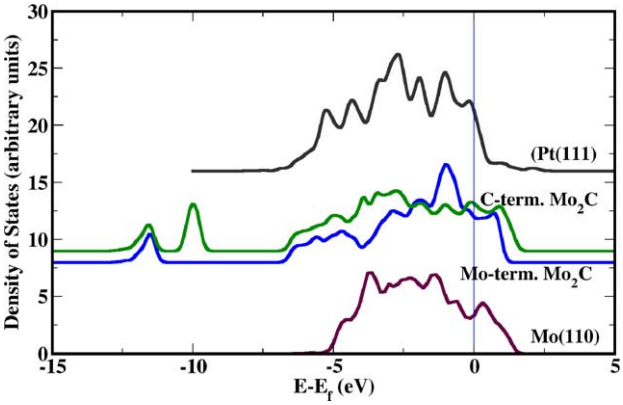

Fig. 1. Comparison of d-band structures of Pt(1 1 1), β-Mo_2C surfaces and Mo(1 1 0).

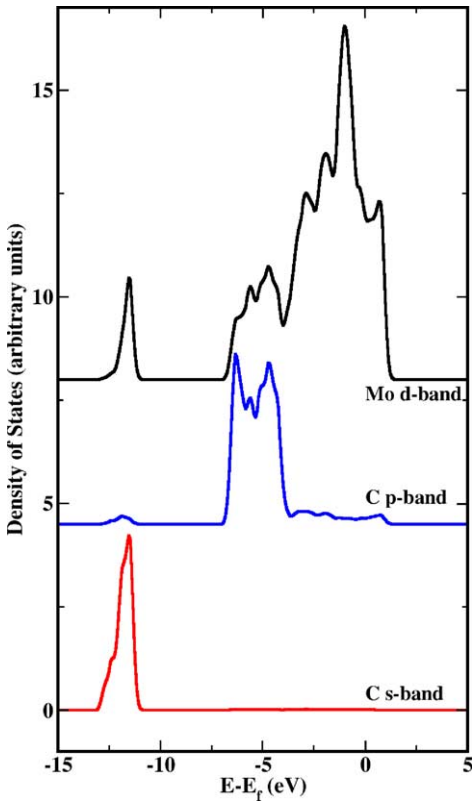

Fig. 2. Illustration of the Mo–C resonances in the β-Mo_2C(0 0 0 1) Mo-terminated surface.

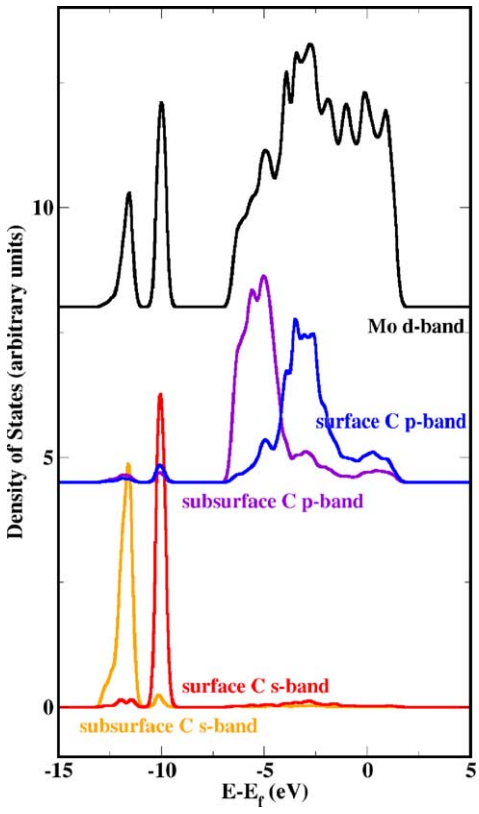

Fig. 3. Illustration of the Mo–C resonances in the β-Mo_2C(0 0 0 1) C-terminated surface. The C atoms in this figure are in the second layer, directly below the surface.

One explanation of the platinum-like catalytic properties observed for some carbides could be a change in the number of d-electrons. Thus, one may consider that C has four valence electrons, which if added to the Mo valence electrons, could increase the d-electron count of Mo to be nearly like the d-electron count of Pt. However, the number of d-electrons in these carbide surfaces, as calculated by integrating the projected density of states up to the Fermi Level (shown in Table 2), is nearly identical to that of the Mo(1 1 0) surface on both Mo- and C-terminated carbide surfaces. The difference is largest on the C-terminated surface, but in our experience this is still too small a difference to be certain of its significance. This suggests that C atoms do not donate their electrons to the Mo d-band to make its electron count more Pt-like. This conclusion is based on orbital population analysis, however, and there are well-known problems with this, such as basis set dependence [11]. Recently Liu and Rodriguez reported charge transfer in the opposite direction, from Mo to C for γ-MoC [12]. In that work, the Mo surface atom became more positive by about half an electron, whereas the subsurface C atom became more negatively charged by about one electron. It is possible this difference is due to the difference in structure and composition between their work and this work. However, their calculations were performed with DMol[3], which uses a localized basis set, and their charge transfer arguments are based on changes in Mulliken orbital populations. Thus, it is likely that these results simply are not directly comparable with ours and are not necessarily in disagreement.

Table 2
Calculated number of d-electrons/surface Mo atom in Mo(1 1 0) and β-Mo_2C(0 0 0 1) (infinite cutoff radius)

Surface	d-Electrons/surface metal atom
Mo(1 1 0)	6.47
Mo-terminated β-Mo_2C(0 0 0 1)	6.45
C-terminated β-Mo_2C(0 0 0 1)	6.69
Pt(1 1 1)	9.26

2.2.1. Adsorption of atomic hydrogen

The adsorption of H atoms on β-Mo_2C(0 0 0 1) was investigated using density functional theory. Adsorption on each three-fold site on both Mo- and C-terminated surface was considered. Adsorption on the terminal and two-fold sites was not considered in this work. The sites are illustrated and labeled in Fig. 4, and the adsorption energy results are listed in Table 3.

The H atom was found to adsorb considerably more strongly on the Mo-terminated surface than on the clean Mo(1 1 0) surface. This was surprising, as we expected the carbide surfaces to be less reactive than the pure metal surfaces. This will be discussed in greater detail in the next section. It is interesting to note that H was unstable on two of the sites. These sites are the ones with a C atom directly

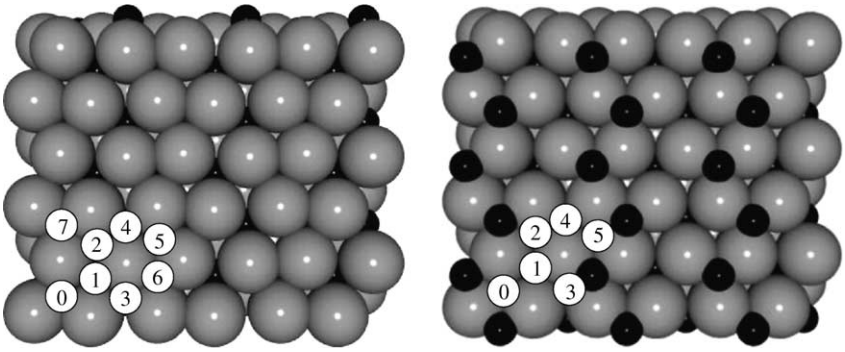

Fig. 4. 3 × 3 Surface unit cells with labeled adsorption sites. Grey atoms are metal, black atoms are carbon.

below them, sites 1 and 4. Hydrogen atoms could still occupy these sites at higher coverages than those examined here, but this was not investigated in this work. None of the adsorption energies on this surface were weaker than those on Mo(1 1 0).

In contrast to the Mo-terminated surface, H atoms were stable on three-fold sites with C atoms directly below them on the C-terminated surface. Two of the sites that were composed of Mo atoms with two surface carbons on them were unstable, sites 0 and 5. The hydrogen on site 5 formed a C–H species that was more stable than any other adsorption site on either surface. Only one site (4) on this surface had a significantly weaker adsorption energy than that on Mo(1 1 0), but it was still more strongly adsorbed than that on Pt(1 1 1). All of the adsorption energies on the C-terminated surface (except the C–H species) are weaker than those on the Mo-terminated surface.

The formation of the C–H species was somewhat surprising. One could argue that it could be expected as C prefers to have four bonds in an sp^3 form, and it is only bonded to three Mo atoms in the surface. However, the C may be bound rather strongly to these three Mo atoms, and a perturbed sp^2 description may be more appropriate. NEXAFS analysis of VC/V(1 1 0) appears to be consistent with the C being more sp^2-like than sp^3-like [13], but a thorough discussion of the difficulties and potential problems with this analysis is also given in the same reference. Thus, it is unclear whether these arguments can be used to determine whether C–H bonding should be expected or not. In the next sections, it will be seen that C–H formation is not limited to β-Mo_2C, but is also seen on the other C-terminated carbide surfaces examined in this work.

Table 3
Calculated hydrogen binding energy (HBE) on Mo- and C-terminated Mo_2C surfaces

Site	Mo-terminated surface HBE (eV)	C-terminated surface HBE (eV)
0	−3.19	Unstable → 1
1	Unstable → 3	−3.00
2	−3.25	Unstable → 4
3	−3.25	−3.00
4	Unstable → 2	−2.83
5	−3.19	Unstable → C–H (−3.36 eV)
6	−3.32	N/A
7	−3.32	N/A
Pt(1 1 1)	−2.66	
Mo(1 1 0)	−3.04	

The numbering scheme is illustrated in Fig. 4.

3. Theoretical studies of Rocksalt carbides

Ti, V, Nb and Ta all form monocarbides with an fcc B1 crystal structure [7]. These crystal structures contain two inter-penetrating fcc lattices, with one lattice containing the metal atoms and the other containing the carbon atoms, similar to the NaCl crystal structure (hence the nomenclature ''rock-salt carbides'' used in this paper). Alternatively, the crystal structure consists of alternating layers of hexagonal close packed metal and carbon atoms in the order M–C–M–C–M–C. In this section we first examine bulk properties of these carbides, and then properties of clean surfaces. When possible the calculated properties are compared to experimentally known properties. Finally, the adsorption properties of H are discussed on these surfaces.

3.1. Bulk properties

The lattice constants and bulk moduli for the carbides were calculated using the Murnaghan equation of state [14], and are listed in Table 4. The bulk moduli for the rocksalt carbides are listed in Table 5. In all calculations, a 400 eV planewave cutoff was used with a 4 × 4 × 4 Monkhorst Pack k-point grid, and the PW91 exchange-correlation functional. The experimental data is taken from Ref. [1] and except for the VC bulk modulus, are results from single-crystals. For VC, the bulk modulus was estimated from the

Table 4
Experimental [7] and calculated lattice constants for rocksalt carbides

	Experimental (Å)	Calculated (Å)	Error (%)
TiC	4.328	4.332	0.09
VC	4.165	4.156	−0.002
NbC	4.470	4.483	0.003
TaC	4.455	4.468	0.003

Table 5
Experimental [1] and calculated bulk moduli for rocksalt carbides

	Experimental (Mbar)	Calculated (Mbar)	Error (%)
$TiC_{0.91}$	2.41	2.51	4.01
VC (polycrystalline)	2.59	2.93	13.1
$NbC_{0.964}$	3.03	1	−1.44
$TaC_{0.994}$	3.45	3.25	−5.73

Calculated values are for stoichiometric carbides.

Table 6
Comparison of experimental [3] and calculated layer spacings for metal-terminated (1 1 1) rocksalt carbide surfaces

	Experimental d_b (Å)	Calculated d_b (Å)	Experimental $-\Delta_{12}$ (Å)	Calculated $-\Delta_{12}$ (Å)
TiC(1 1 1)	1.25	1.25	0.38	0.23
VC(1 1 1)	1.21	1.20	0.12	0.22
NbC(1 1 1)	1.29	1.29	0.20	0.20
TaC(1 1 1)	1.29	1.29	0.15	0.16

reported value of the Young's modulus of a polycrystalline sample using the following equation:

$$B = \frac{Y}{3(1-2\nu)} \quad (1)$$

where B is the bulk modulus, Y the Young's modulus, and ν is the Poisson's ratio. The agreement between the theoretical calculations and experimentally reported values is quite reasonable. The calculated lattice constant and bulk modulus from this work for TiC are in quantitative agreement with other published results [15,16]. Finally, the trend in the heats of formation was also correctly described by our calculations.

3.2. Surface properties

The rocksalt carbide(1 1 1) surface can be either metal or carbon-terminated, as shown in Fig. 5. One significant difference between the C-terminated rocksalt carbide surfaces and those of the β-Mo_2C(0 0 0 1) is that there is a full monolayer of C on the rocksalt carbide surfaces, and all of the remaining three-fold sites are equivalent. The surfaces were represented by four metal–carbon layers, with two of the layers being frozen at the bulk lattice parameters, and the other two allowed to relax. A planewave cut-off of 400 eV was used. The PW91 exchange-correlation functional and a $4 \times 4 \times 1$ Monkhorst-Pack k-point setup was used in all calculations. The slabs were separated by 12 interlayer spacings of vacuum, which was typically about 14 Å.

The real structure of a surface is rarely identical to that of an ideal, bulk-terminated surface because the surface atoms are no longer in the same electronic environment as the bulk atoms. Consequently, the surface layers tend to relax, either inward or outward, to minimize the surface energy. Johannson summarized the findings of several surface science studies on the (1 1 1) rocksalt carbide surfaces [3], and reported a contraction in the first interlayer spacing for these rocksalt carbides. In Table 6, the calculated changes in interlayer spacing are compared to the experimentally determined interlayer spacing.

Focusing on the first two columns, which are the bulk interlayer spacings, there is excellent agreement between the experimental and calculated values for all of the carbides. This was expected because of the excellent agreement in the bulk lattice constants obtained. The next two columns compare the experimental and calculated spacing between the metal-terminated surface and the carbon layer directly below it. The agreement for NbC(1 1 1) and TaC(1 1 1) is exceptional. The interlayer spacing between the second and third layer for NbC(1 1 1) was also reported as −0.05 Å [3], and is calculated to be +0.03 Å. The signs differ, but the magnitude is so small that it is also considered good agreement. The agreement between theory and experiment for TiC and VC is not as good. The contraction is correctly predicted in each case, but the magnitude is underestimated for TiC(1 1 1) and overestimated for VC(1 1 1). The TiC results were obtained from impact collision ion scattering spectroscopy (ICISS) [17], which was reported in that work to have an accuracy of about ±0.1 Å.

The VC results in Table 6 were from a substoichiometric $VC_{0.80}$(1 1 1) surface in its 1×1 metastable state [18]. The surface was considered metastable because a reconstruction occurs at annealing temperatures above 1000 K. The lattice constant of this substoichiometric carbide was 4.147 Å, compared to 4.182 Å for stoichiometric VC [18]. The authors in that work determined the composition of the first four layers to be stoichiometric, i.e. VC, using LEED. Thus, the top layers

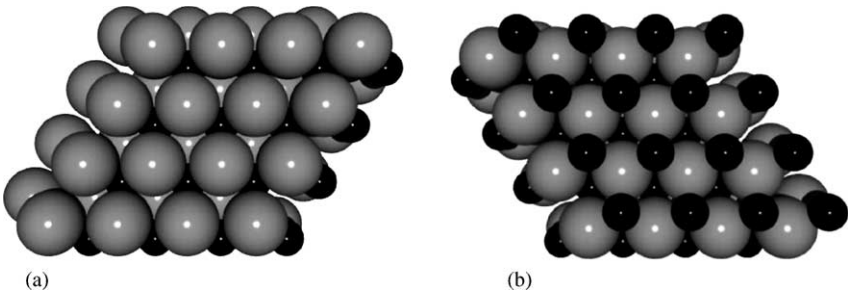

Fig. 5. Possible terminations of the (1 1 1) rocksalt carbide surface. Grey atoms are metal, black atoms are carbon. (a) Metal terminated (1 1 1) surface. (b) Carbon terminated surface (1 1 1).

of the experimental surface could be considered to be laterally (compressively) strained due to the C enrichment compared to layers deeper in the bulk. This could result in less contraction of these layers, due to the extra coordination the excess carbon would provide. The calculated results in this work for a stoichiometric surface would then appear to overestimate the experimentally reported contraction. Calculations on a $VC_{0.80}$(1 1 1) surface are presently unfeasible, as a very large unit cell would be required to represent the stoichiometry and to ensure the carbon defects do not interact. According to the LEED studies of Rundgren et al. [18], one would also have to consider gradients in the carbon vacancy concentration in the unit cell. We are unaware of any similar experimental results reported on stoichiometric VC(1 1 1).

In conclusion, the DFT calculations performed on rocksalt carbide bulk and surfaces in this work correctly predicted a range of physical properties, from lattice constants and bulk moduli, to contraction of the interlayer spacings on the metal-terminated surfaces, in some cases with quantitative agreement with experimental results. While these are not directly chemical properties, which are discussed next, these results do indicate that DFT at the level we have applied has thus far been sufficient to model the properties we have investigated.

3.2.1. Adsorption of atomic hydrogen

The adsorption of hydrogen atoms was considered on both the metal and carbon-terminated surfaces. On the metal-terminated surface, only the three-fold site without a carbon underneath it was considered, since the sites with subsurface C under them in the β-Mo_2C work were found to be unstable.

The hydrogen binding energy (HBE) values on the metal-terminated carbide surface and the ground state pure metal surface (hcp(0 0 01) or bcc(1 1 0)) are compared in Fig. 6. As seen for β-Mo_2C, H adsorbs more strongly to the metal-terminated carbide surface than to the corresponding pure metal surface, with the exception of VC. We do not presently have an explanation for the apparent different behavior of VC compared to the other carbides.

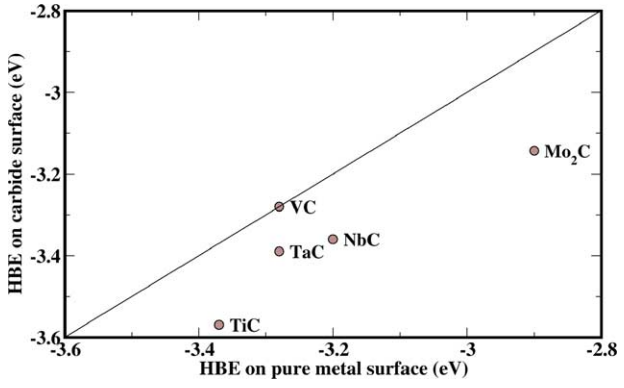

Fig. 6. Comparison of the HBE on metal-terminated carbide surfaces with the HBE on pure bcc metal surfaces.

Table 7
Nearest neighbor distances for early transition metals and carbides

Pure metal	Nearest neighbor distance (Å)	Metal carbide	Nearest neighbor distance (Å)
Ti	2.89	TiC	3.06
V	2.62	VC	2.95
Nb	2.86	NbC	3.16
Ta	2.86	TaC	3.15
Mo	2.73	Mo_2C	3.04

One reason for the stronger adsorption energies on the carbide surfaces may be that compared to the pure metal surfaces, the carbide surfaces are all under tensile strain. Table 7 compares the nearest neighbor distances in the pure metals to those in the carbides, where it is seen that the metal atoms in the carbide are farther apart than in the pure metals. Neglecting the effect that the subsurface C could have, this means that the surface atoms are under-coordinated in the metal-terminated carbide surface compared to the surface atoms of the pure metal, which could explain why H atoms bind more strongly to the metal-terminated carbide surface. Late transition metal surfaces under tensile strain also exhibit stronger adsorption energies for atomic and small molecular adsorbates [19]. The subsurface C atoms are expected to attenuate this effect.

H atoms were not stable on the three-fold sites of any of the C-terminated carbide surfaces, in each case forming a very stable C–H bond. On TaC(1 1 1), the heat of adsorption was calculated to be −3.92 eV, which is substantially higher than on the metal sites. The high heat of adsorption suggests that these C–H species should exist on C-terminated carbide surfaces, analogous to OH species on oxide surfaces. A complete discussion of these C–H species is beyond the scope of this paper, and they are not considered further. We did not determine the adsorption energy of a hydrogen atom in a three-fold site after all surface C atoms had been capped by H.

A major motivation of this work was to determine if the d-band center model [20,21] for adsorption that we have successfully used in describing H adsorption on bimetallic surfaces [22–24] could also be used to describe H adsorption on carbide surfaces. With the bimetallic surfaces, it was found that either the short or infinite d-band center could be used in correlations with adsorption energies. This was due to the fact that these two moments were highly correlated with each other. In the carbide surfaces, however, these moments were not as strongly correlated, and very little correlation was found between the infinite d-band center and the HBE for these carbide surfaces. One potential issue with the infinite cutoff radius is that it can overcount electrons from nearby atoms. Thus, the projection could be including electrons that should be associated more with the C atoms than the metal atoms. This is an intrinsic problem in any density-partitioning scheme. The partitioned density does not correspond to a physical observable, and the details of its implementation are largely arbitrary. The problem with including the C-states is that they lower the d-band center

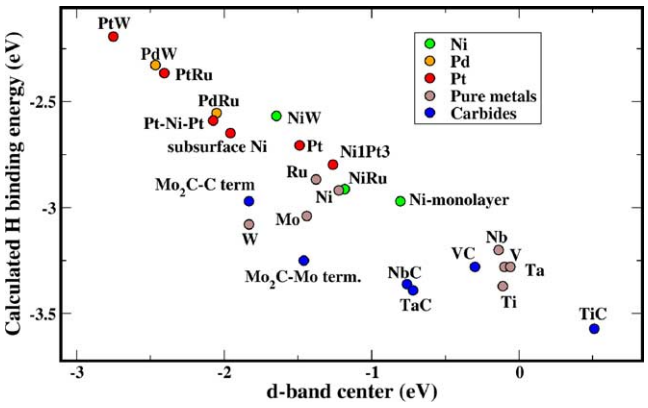

Fig. 7. Correlation between the short d-band center and HBE on epitaxial transition metal monolayers, bimetallic sandwich structures, surface alloys, early transition metal and carbide surfaces. The bimetallic data can be found in references [22–24]. The pure metal surfaces correspond to the closest-packed surface for the parent metal crystal structure (fcc(1 1 1), bcc(1 1 0), hcp(0 0 1)).

substantially because they are so low in energy. However, because they are so low in energy, it is unlikely these states play a significant role in H adsorption.

The intensity of the C-derived states is considerably lower in the projected DOS that has been cut off at 1 Å than in the infinite cutoff radius projection, and the d-band center of this projection is correspondingly higher in energy. The correlation between the HBE and the short d-band center is substantially improved compared to correlation with the infinite d-band center, and is shown in Fig. 7. Obviously the correlation is not as good as the one found for the bimetallic systems (also shown in Fig. 7), but it clearly follows the trend.

Aside from the difficulties in describing the d-band structure of the carbides discussed above, there are additional reasons why the correlation may not be as good as that observed for bimetallic surfaces. The correlation between the d-band center and the adsorption energy is the simplest version of the d-band model [20,21], in which variations in the matrix elements and the shape of the bands have been neglected. It is therefore not surprising that distortions of the band shape due to the interaction with carbon can modify the correlation. It is also clear that direct interactions with the C atoms cannot be excluded in all cases. There is ample scope for more work in this area.

4. Conclusions

It has been demonstrated that DFT can be used effectively to study transition metal carbide surfaces. Calculated bulk properties compared very well to experimentally reported values, with lattice constants typically being within 2%, and bulk moduli typically within 5% of experimental values. The trend in the heats of formation was also correct. On the carbide surfaces, in all cases the contraction in the interlayer spacing of the first layer was qualitatively correct, and in many cases was quantitatively correct.

Hydrogen was found generally to adsorb more strongly to the close-packed metal-terminated carbide surfaces than to the corresponding pure metal(1 1 0) surfaces or carbon-terminated carbide surfaces. The higher adsorption energy on the metal-terminated carbide surfaces was attributed to the tensile strain induced by incorporation of carbon atoms into the metal lattice. Most significantly, it was found that the hydrogen adsorption energy could be correlated with the d-band center of the carbide surface, provided that the contributions of the d-states resulting from hybridization with the non-bonding C s states were minimized.

On carbon-terminated surfaces, hydrogen was found to adsorb more weakly to some sites of β-Mo_2C(0 0 0 1) than to Mo(1 1 0). This suggests that C-termination may be required to obtain a surface reactivity that is less active than that of the parent metal, and that the surface C-atoms have a passivating role. This is suggestive that defect chemistry can be important, since defect sites may have differing levels of C-passivation, and thus different levels of chemical reactivity. On all C-terminated surfaces considered, stable C–H species were readily formed, suggesting that these carbons may be chemically active. It has been reported in other theoretical studies that surface C atoms may take part in the desulfurization of SO_2 on TiC(0 0 1) [25], and that isocyanate species (−N=C=O) can form from CO and surface N atoms on molybdenum nitride surfaces [26]. Thus, these C and N atoms may serve as more than site blockers.

In conclusion, studies of transition metal carbide surfaces are more complex than those of pure metal surfaces, as issues of surface termination, a multitude of different possible sites, and the possibility that defect chemistry is significant must be considered. It is correspondingly more difficult to directly compare theoretical calculations to experimental results due to the difficulties involved with characterization of the surfaces. However, with carefully planned sets of calculations, trends can readily be studied, which can then be used to help interpret experimental findings and to design new experiments.

Acknowledgements

This work was funded in part by Basic Energy Sciences, Department of Energy (Grant DE-FG02-04ER15501). JRK acknowledges the National Science Foundation Graduate Research Fellowship program. The Center for Atomic-scale Materials Physics is sponsored by the Danish National Research Foundation. The DFT calculations have been performed with support from the Danish Center for Scientific Computing through grant no. HDW-1101-05.

References

[1] L.E. Toth, Transition metal carbides and nitrides, Refractory Materials: A Series of Monographs, vol. 7, Academic Press, 1971.

[2] R.B. Levy, M. Boudart, Science 181 (1973) 547–549.
[3] L.I. Johannson, Surf. Sci. Rep. 21 (1995) 177–250.
[4] S.T. Oyama (Ed.), The Chemistry of Transition Metal Carbides and Nitrides, Blackie Academic & Professional, 1996.
[5] J.G. Chen, Chem. Rev. 96 (1996) 1477–1498.
[6] H.H. Hwu, J.G. Chen, Chem. Rev. 105 (2005) 185–212.
[7] H. Tulhoff, H.C.S. Berlin, W. Goslar, Carbides, in: W. Gerhartz, Y.S. Yamamoto, F.T. Campbell, R. Pfefferkorn, J.F. Rounsav-ille (Eds.), fifth ed. (completely revised), Ullmann's Encyclopedia of Industrial Chemistry, vol. A5, Wiley–VCH Verlag GmbH & Co., 2000 pp. 61–77.
[8] B.V. Khaenko, O.A. Gnitetskii, V.Z. Kublii, Dopovidi Akademii Nauk Ukrains'koi RSR, Seriya A: Fiziko-Tekhnichni ta Matematichni Nauki, 1991 pp. 78–82.
[9] http://www.fysik.dtu.dk/CAMPOS.
[10] P. Liu, J.A. Rodriguez, J.T. Muckerman, J. Phys. Chem. B 108 (2004) 15662–15670.
[11] W. Koch, M.C. Holthausen, A Chemist's Guide to Density Functional Theory, second ed., Wiley–VCH, 2001.
[12] P. Liu, J.A. Rodriguez, Catal. Lett. 91 (3–4) (2003) 247–252.
[13] J.G. Chen, C.M. Kim, B. Friiberger, B.D. DeVries, M.S. Touvelle, Surf. Sci. 321 (1994) 145–155.
[14] C.-L. Fu, K.-M. Ho, Phys. Rev. B 28 (10) (1983) 5480–5486.
[15] S.V. Dudiy, B.I. Lundqvist, Phys. Rev. B 64 (2001) 045403.
[16] L.M. Liu, S.Q. Wang, H.Q. Ye, J. Phys.: Condens. Matter (8103–8114) (2003).
[17] M. Aono, C. Oshima, S. Zaima, S. Otani, Y. Ishizawa, Jpn. J. Appl. Phys. 20 (11) (1981) L829–L832.
[18] J. Rundgren, Y. Gauthier, R. Baudoing-Savois, Y. Joly, L.I. Johansson, Phys. Rev. B 45 (8) (1992) 4445–4453.
[19] M. Mavrikakis, B. Hammer, J.K. Nørskov, Phys. Rev. Lett. 81 (13) (1998) 2819–2822.
[20] B. Hammer, J.K. Nørskov, Nature 376 (1995) 238–240.
[21] B. Hammer, J.K. Nørskov, Surf. Sci. 343 (1995) 211–220.
[22] J.R. Kitchin, N.A. Khan, J.G. Chen, M.A. Barteau, T.E. Madey, B. Yakshinsky, Surf. Sci. 544 (2–3) (2003) 295–308.
[23] J.R. Kitchin, J.K. Nørskov, J.G. Chen, M.A. Barteau, J. Chem. Phys. 120 (21) (2004) 10240–10247.
[24] J.R. Kitchin, J.K. Nørskov, M.A. Barteau, J.G. Chen, Phys. Rev. Lett. 93 (2004) 156801.
[25] J.A. Rodriguez, P. Liu, J. Dvorak, T. Jirsak, J. Gomes, Y. Takahashi, K. Nakamura, Surf. Sci. 543 (2003) L675–L682.
[26] G. Frapper, M. Pelissier, J. Hafner, J. Phys. Chem. B 104 (2000) 11972–11976.